ACCOUNTS of chemical research

Article

pubs.acs.org/accounts

Highly Efficient Bioinspired Molecular Ru Water Oxidation Catalysts with Negatively Charged Backbone Ligands

Published as part of the Accounts of Chemical Research special issue "Synthesis in Biological Inorganic Chemistry".

Lele Duan,[§] Lei Wang,[§] Fusheng Li,[§] Fei Li,[¶] and Licheng Sun*[,§,¶]

[§]Department of Chemistry, School of Chemical Science and Engineering, KTH Royal Institute of Technology, SE-100 44 Stockholm, Sweden

[¶]State Key Lab of Fine Chemicals, Institute of Artificial Photosynthesis, DUT-KTH Joint Education and Research Center on Molecular Devices, Dalian University of Technology (DUT), 116024 Dalian, China

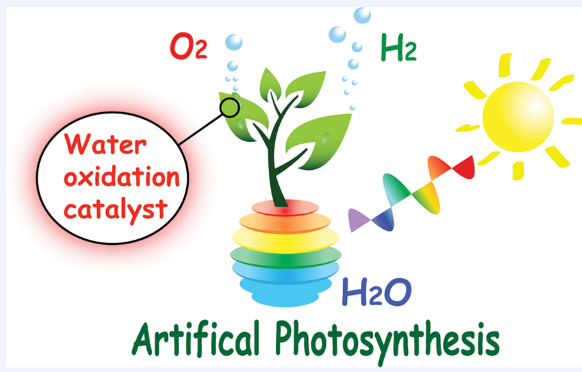

CONSPECTUS: The oxygen evolving complex (OEC) of the natural photosynthesis system II (PSII) oxidizes water to produce oxygen and reducing equivalents (protons and electrons). The oxygen released from PSII provides the oxygen source of our atmosphere; the reducing equivalents are used to reduce carbon dioxide to organic products, which support almost all organisms on the Earth planet. The first photosynthetic organisms able to split water were proposed to be cyanobacteria-like ones appearing ca. 2.5 billion years ago. Since then, nature has chosen a sustainable way by using solar energy to develop itself. Inspired by nature, human beings started to mimic the functions of the natural photosynthesis system and proposed the concept of artificial photosynthesis (AP) with the view to creating energy-sustainable societies and reducing the impact on the Earth environments. Water oxidation is a highly energy demanding reaction and essential to produce reducing equivalents for fuel production, and thereby effective water oxidation catalysts (WOCs) are required to catalyze water oxidation and reduce the energy loss.

X-ray crystallographic studies on PSII have revealed that the OEC consists of a Mn_4CaO_5 cluster surrounded by oxygen rich ligands, such as oxyl, oxo, and carboxylate ligands. These negatively charged, oxygen rich ligands strongly stabilize the high valent states of the Mn cluster and play vital roles in effective water oxidation catalysis with low overpotential. This Account describes our endeavors to design effective Ru WOCs with low overpotential, large turnover number, and high turnover frequency by introducing negatively charged ligands, such as carboxylate. Negatively charged ligands stabilized the high valent states of Ru catalysts, as evidenced by the low oxidation potentials. Meanwhile, the oxygen production rates of our Ru catalysts were improved dramatically as well. Thanks to the strong electron donation ability of carboxylate containing ligands, a seven-coordinate Ru^{IV} species was isolated as a reaction intermediate, shedding light on the reaction mechanisms of Ru-catalyzed water oxidation chemistry. Auxiliary ligands have dramatic effects on the water oxidation catalysis in terms of the reactivity and the reaction mechanism. For instance, Ru-bda (H_2bda = 2,2′-bipyridine-6,6′-dicarboxylic acid) water oxidation catalysts catalyze Ce^{IV}-driven water oxidation extremely fast via the radical coupling of two Ru^V═O species, while Ru-pda (H_2pda = 1,10-phenanthroline-2,9-dicarboxylic acid) water oxidation catalysts catalyze the same reaction slowly via water nucleophilic attack on a Ru^V═O species. With a number of active Ru catalysts in hands, light driven water oxidation was accomplished using catalysts with low catalytic onset potentials. The structures of molecular catalysts could be readily tailored to introduce additional functional groups, which favors the fabrication of state-of-the-art Ru-based water oxidation devices, such as electrochemical water oxidation anodes and photo-electrochemical anodes. The development of efficient water oxidation catalysts has led to a step forward in the sustainable energy system.

■ INTRODUCTION

Currently the world energy supply is mainly based on burning fossil fuels, which leads to serious global environmental problems, such as greenhouse effect, pollution, and energy crises. The development of sustainable energy systems is urgently required. Inspired by natural photosynthesis, human beings proposed the concept of artificial photosynthesis (AP) to create energy-sustainable societies by converting infinite and nonpolluting solar energy to fuels. In general, AP consists of two types of reactions: the water oxidation reaction ($2H_2O \rightarrow 4H^+ + 4e^- + O_2$) and reduction reactions (such as proton reduction and CO_2 reduction). Regardless which type of reduction reaction is considered, water oxidation is considered as the bottleneck of artificial photosynthesis, due to its highly energy demanding profile (E = 1.23 − 0.059 × pH V vs NHE); meanwhile,

Received: March 25, 2015
Published: July 1, 2015

 © 2015 American Chemical Society

DOI: 10.1021/acs.accounts.5b00149
Acc. Chem. Res. 2015, 48, 2084−2096

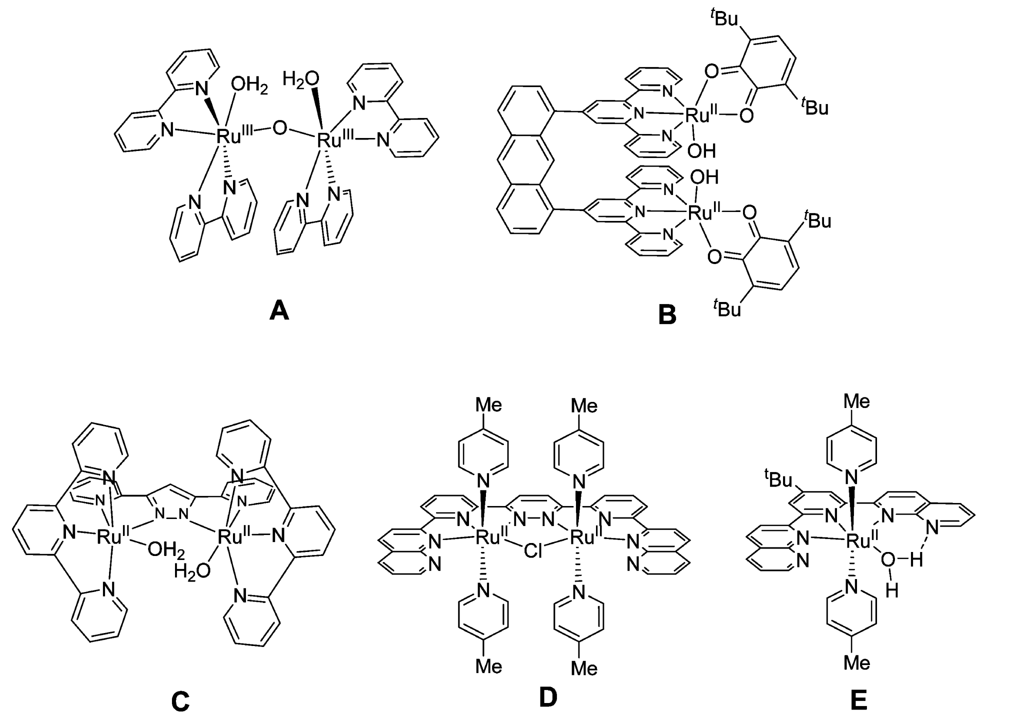

Figure 1. Structures of complexes **A**−**E**.

overpotential is always present in reality, leading to higher potentials than the thermodynamic values. Thereby, effective water oxidation catalysts (WOCs) are required for efficient solar energy to fuel conversion processes.

■ THE OXYGEN EVOLVING COMPLEX

The oxygen evolving complex (OEC) in photosystem II (PSII) is the active center of water oxidation in nature. It oxidizes water to oxygen with low overpotential (20 mV) and high activity (100−400 turnovers per second in vivo).[1,2] The OEC consists of a cubane-like Mn_4CaO_5 cluster with six carboxylate ligands (amino-acid residues), one imidazole (His332), and four aqua ligands.[3] The presence of *oxo* and *carboxylate ligands* is crucial for lowering the oxidation potentials of the OEC, holding the Mn cations at proper positions, and transporting protons generated during water oxidation. The OEC has provided scientists a blueprint of how to design effective WOCs. However, a replication of the OEC is extremely difficult due to its complex surrounding proteins. Thereby, we have sought to develop simple transition metal complexes as bioinspired molecular catalysts for water oxidation by introducing negatively charged ligands, such as *carboxylate*-containing ligands.

■ THE STARTING POINT

When we started to study Ru-based WOCs, there were only five families of molecular Ru complexes (**A**−**E**; Figure 1) in the literature capable of catalyzing water oxidation using either electrical or chemical power.[4−6] Thummel's complexes **D** and **E** exhibit large turnover numbers (TONs) and turnover frequencies (TOFs) toward Ce^{IV}-driven water oxidation (eq 1); however, those Ru complexes exhibit relatively high oxidation potentials and catalytic onset potentials.

$$2H_2O + 4Ce^{IV} \xrightarrow{\text{catalyst}} O_2 + 4H^+ + 4Ce^{III} \quad (1)$$

We decided to increase the electron donating ability of the npp (Figure 2) ligand by removing two electron withdrawing pyridine motifs and installing electron donating alkyl groups. Ligands Mebpp and bcd, as well as their corresponding Ru complexes **1**, **2** and **3**, were prepared (Figure 2).[7] Due to the weak electron donating ability of alkyl groups, the resulting Ru complexes did not show much lower oxidation potentials than **D**. Nevertheless, better catalytic activity toward Ce^{IV}-driven water oxidation was observed for both **1** and **2** in comparison with **D**.

■ BINUCLEAR Ru COMPLEXES WITH CARBOXYLATE-CONTAINING LIGANDS: MOVING TO THE RIGHT TRACK

Stronger electron donating ligands than alkyl groups are required to significantly reduce the oxidation potentials of Ru WOCs; meanwhile they have to be resistant to oxidative decomposition. Starting in the 1990s, Sun, Åkermark, and their coworkers synthesized a series of Ru−Mn complexes.[8] Particularly, a trinuclear Ru/Mn_2 complex (**Ru−Mn$_2$**, Figure 3) successfully achieved light-driven multiple electron transfer, resulting in stepwise oxidation of $Mn_2^{II,II} \rightarrow Mn_2^{II,III} \rightarrow Mn_2^{III,III} \rightarrow Mn_2^{III,IV}$, thanks to the strong electron donating properties of phenolate and carboxylate ligands, which stabilize the high valent Mn cations and lower the oxidation potentials of **Ru−Mn$_2$**.[9] This was reminiscent of the oxygen rich environment of the OEC. Accordingly, a carboxylate-containing ligand, 3,6-bis(6′-COOH-pyrid-2′-yl)pyridazine (H_2cppd; Figure 4), was designed. Complexation of H_2cppd with *cis*-[Ru(dmso)$_4$Cl$_2$] (dmso = dimethyl sulfoxide) in the presence of base and subsequent treatment with excess 4-picoline (pic) leads to the formation of an unexpected *anti*-binuclear Ru complex [Ru$_2$(cppd−H)(pic)$_6$]-(PF$_6$) (**4**; Figure 4).[10]

Two reversible couples at $E_{1/2}(Ru_2^{II,III/II,II})$ = 0.29 and $E_{1/2}(Ru_2^{III,III/III,II})$ = 0.80 V versus SCE were observed for **4**, which are respectively decreased by 0.96 and 0.86 V in comparison

DOI: 10.1021/acs.accounts.5b00149
Acc. Chem. Res. 2015, 48, 2084−2096

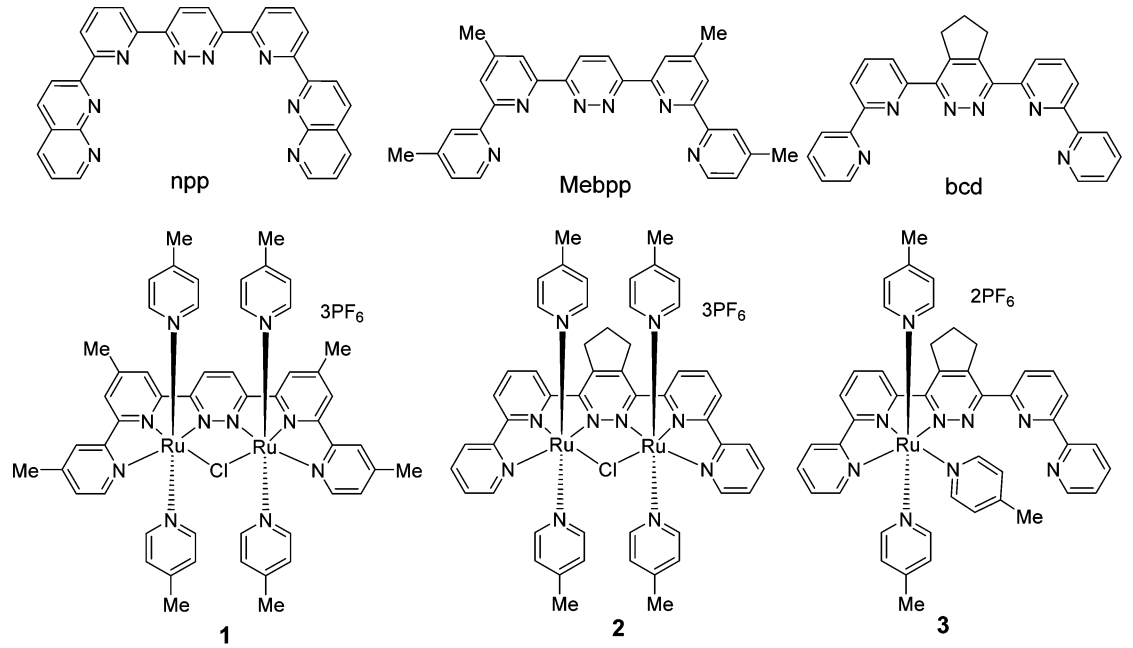

Figure 2. Structures of complexes **1**−**3** and ancilary ligands npp, Mebpp, and bcd.

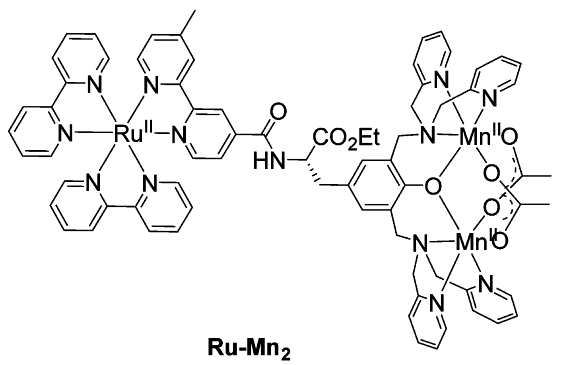

Figure 3. Molecular structure of **Ru**−**Mn$_2$**.

with **D** ($E^{ox}_{1/2}$ = 1.25 and 1.66 V versus SCE). For Ce^{IV}-driven water oxidation, the TON and TOF of **4** (1700, 0.28 s^{-1}) have been improved by three and five times, respectively, compared with those of **D** (538, 0.046 s^{-1}) under the same conditions.

To avoid the formation of the Ru−C bond in **4**, a new ligand 1,4-bis(6′-COOH-pyrid-2′-yl)phthalazine (H_2bcpp; Figure 5) in which the central pyridazine was replace by a phthalazine motif was designed. In comparison with H_2cppd, H_2bcpp bears an extra phenyl ring that blocks the 4,5-positions of the pyridazine moiety, leading to the formation of the desired *cis*-dinulcear complex **5**.[11]

The TONs of both **4** and **5** increase with the decrease of the Ce^{IV} concentration, most likely due to the oxidative decomposition of the catalyst at high Ce^{IV} concentrations. The *cis*-binuclear complex **5** (TON = 10400) displayed a far superior activity than complex **4** (TON = 4700) *under optimized conditions*. The rate of water oxidation by **5** was found to be first order in the catalyst concentration with a $TOF_{initial}$ = 1.2 s^{-1}.

■ MONONUCLEAR Ru COMPLEXES WITH STRONG ELECTRON DONATING LIGANDS: REDUCING THE COMPLEXITY

Water oxidation mechanisms are complex because of multiple proton/electron transfer steps and several bond cleavage and formation steps. The structural complexity of dinuclear Ru WOCs makes the mechanistic study even more challenging. In comparison, mononuclear Ru WOCs can reduce the complexity for a mechanistic study.

The Ru−O_2N−N_3 Complex

The two Ru centers of complex **4** are linked by the bridging ligand $[cppd-H]^{3-}$, and due to the *anti*-structure, their distance is noticeably longer than that in **D**. The synergistic effect for **4** does not seem to be obvious. In addition, mononuclear Ru complexes, such as complex **E** (Figure 1), can catalyze water oxidation. We thereby designed and synthesized a family of mononuclear Ru complexes **6**−**8** (Figure 6) containing a structurally simple tridentate pdc^{2-} (H_2pdc = 2,6-pyridinedicarboxylic acid) backbone ligand.[12,13]

Their catalytic and electrochemical data are summarized in Table 1. High reaction rates (0.09−0.29 s^{-1}) and TONs (460−560 over 5 h) were obtained for complexes **6a**−**c**. Complex **6d** with electron withdrawing pyrazine exhibited low TOF and TON values. No oxygen was detected for complexes **8a**−**b**. Electron donating groups obviously increase the activity of Ru-pdc complexes.

Mechanistic studies using **6b** as a model complex uncovered that the anionic carboxylate ligand facilitates dissociation of the equatorial 4-picoline, and the resulting equatorial site is essential for the high reactivity of **6b**. When the labile equatorial position was blocked by a bpy (bpy = 2,2′-bipyridine) ligand as in complex **7**, negligible activity was observed. In addition, two reaction intermediates, $[Ru^{III}(pdc)(pic)_2(sol)]^+$ and $[Ru^{III}(pdc)(pic)(sol)_2]^+$ (sol = solvent), were isolated from the catalytic system of **6b**, and the former one was proposed as the real WOC.

Another example of a mononuclear Ru WOC is $[Ru(hqc)(pic)_3]$ (**9**; H_2hqc = 8-hydroxyquinoline-2-carboxylic acid; Figure 7) with hqc^{2-} as a stronger electron donating ligand (due to the strong pπ−dπ interaction between oxygen and ruthenium) than pdc^{2-}.[14] The Ru−hqc catalyst, as expected, has lower oxidation potentials than the Ru−pdc catalysts. The oxygen production rate is first order in catalyst concentration with a $TOF_{initial}$ of 0.32 s^{-1}. Similar to the Ru−pdc catalysts,

DOI: 10.1021/acs.accounts.5b00149
Acc. Chem. Res. 2015, 48, 2084−2096

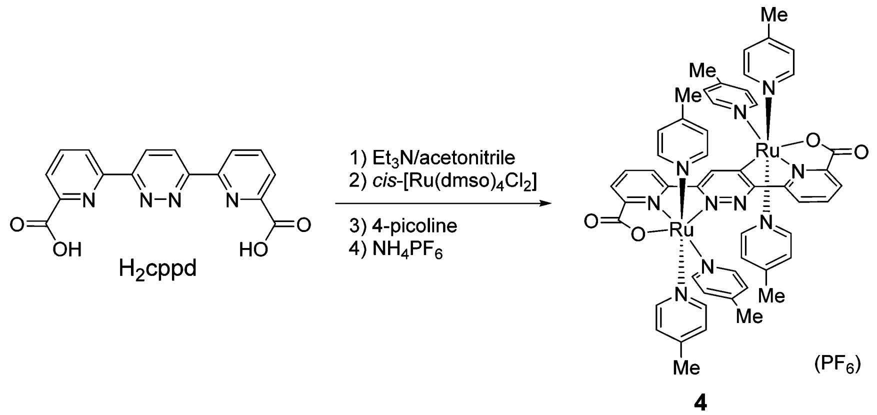

Figure 4. Schematic illustration of the synthesis of **4**.

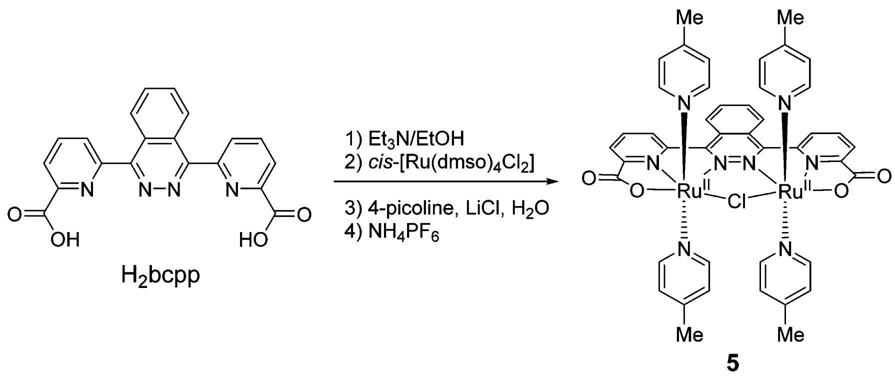

Figure 5. Schematic illustration of the synthesis of **5**.

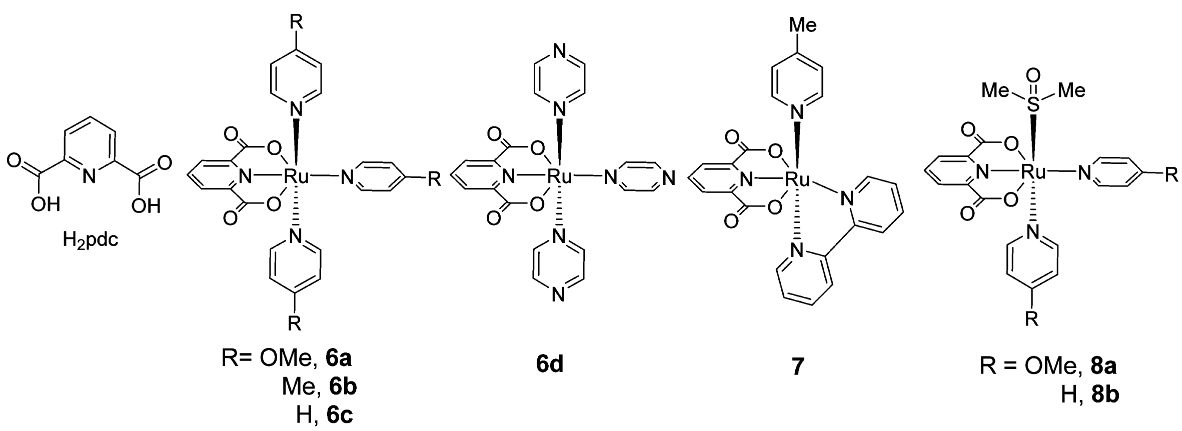

Figure 6. Structures of H_2pdc and complexes **6**−**8**.

Table 1. Catalytic and Electrochemical Data of Complexes 6a−d

complex	E^{ox} (V)	TON	$TOF_{initial}$ (s^{-1})
6a	0.38, 1.21	560	0.29
6b	0.53, 1.22	550	0.23
6c	0.58, 1.24	460	0.09
6d	0.83, 1.30	50	

$[Ru^{III}(hqc)(pic)_2(sol)]^+$ was also observed upon oxidation of **9** (Figure 7). Density functional theory (DFT) calculations suggested a dissociative pathway for the formation of $[Ru^{III}(hqc)(pic)_2(sol)]^+$ via a five-coordinated Ru^{III} intermediate $[Ru^{III}(hqc)(pic)_2]^+$. The required energy of activation for 4-picoline dissociation is calculated to be 12.7 and 12.2 kcal/mol for **6b** and **9**, respectively, which are dramatically lower than that for $[Ru(tpy)(pic)_3]^{2+}$ (**12**; 22.8 kcal/mol; tpy = 2,2′:6′,2″-terpyridine).

The Ru−ON_2−N_3 Analogues

The as-prepared Ru^{II}−pdc and −hqc complexes are usually neutral in charge and insoluble in water, which obstructs the insightful study into the reaction mechanisms. Therefore, the Ru−bpc (Hbpc = 2,2′-bipyridine-6-carboxylic acid) WOCs $[Ru^{II}(bpc)(bpy)(OH_2)]^+$ (**10**) and $[Ru^{II}(bpc)(pic)_3]^+$ (**11**; Figure 8)[15] were prepared to overcome the insolubility issue and exploit the effect of the anionic ligand on catalytic activity. Similar to complexes **6** and **9**, pic/H_2O exchange is required for **11** prior oxidation of water.

Detailed reaction mechanistic studies on complex **10** at pH 1.0 illustrated a catalytic cycle as shown in Figure 9.

DOI: 10.1021/acs.accounts.5b00149
Acc. Chem. Res. 2015, 48, 2084−2096

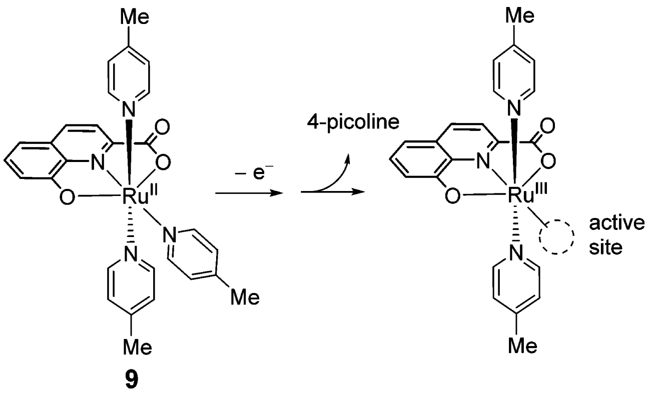

Figure 7. Illustration of the formation of the real catalyst from complex **9**.

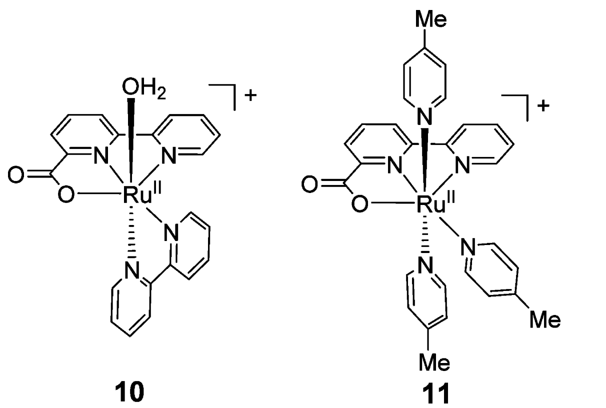

Figure 8. Structures of complexes **10** and **11**.

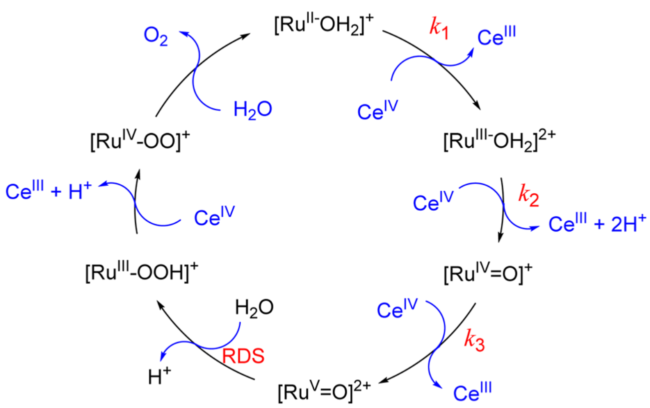

Figure 9. Proposed catalytic cycle of water oxidation catalyzed by **10**.

The $[Ru^{II}{-}OH_2]^+$ is first oxidized to $[Ru^{III}{-}OH_2]^{2+}$, followed by a $2H^+/1e^-$ PCET oxidation step affording $[Ru^{IV}{=}O]^+$. $[Ru^{IV}{=}O]^+$ is not reactive toward water and thereby has to be further oxidized to generate the active species $[Ru^{V}{=}O]^{2+}$. Thereafter, water nucleophilic attack on the Ru^{V} oxo occurs, forming the hydroperoxo intermediate $[Ru^{III}{-}OOH]^+$, which is the rate-determining step (RDS). Finally, another oxidation step takes place and oxygen evolves from $[Ru^{IV}{-}OO]^+$. Interestingly, the anionic ligand bpc^- enhances ET (electron transfer) steps, such as k_1 and k_3 but does not obviously influence the PCET reaction rate (k_2). In comparison with the data of $[Ru(tpy)(bpy)(OH_2)]^{2+}$ and $[Ru(tpy)(bpm)(OH_2)]^{2+}$ (bpm = 2,2′-bipyrimidine), the anionic ligand lowers the oxidation potentials of Ru complexes but increases the pK_a of the corresponding

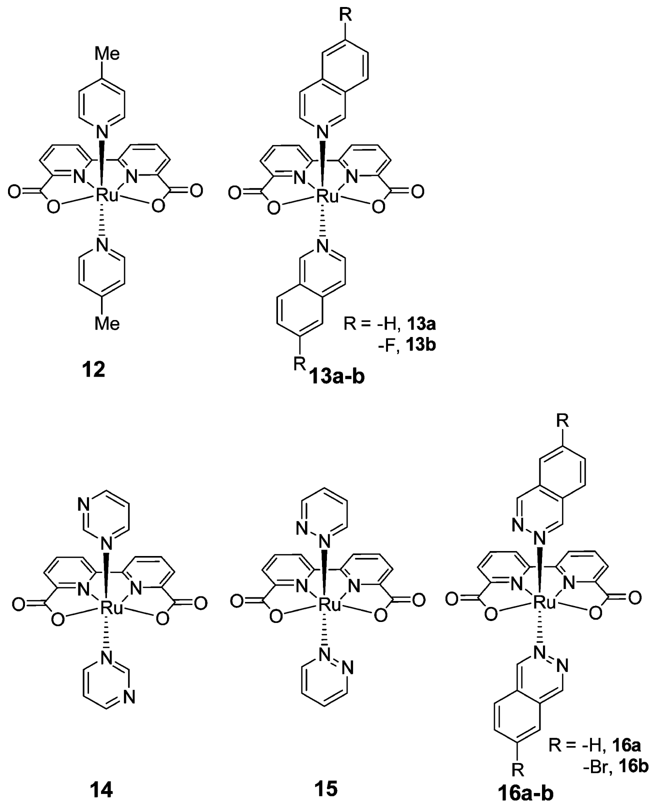

Figure 10. Chemical structures of Ru–bda WOCs mentioned in this Account.

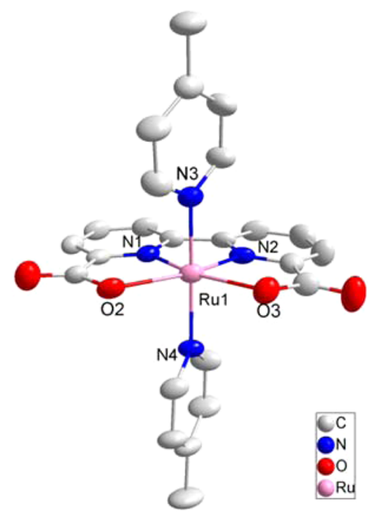

Figure 11. Crystal structure of complex **12** with thermal ellipsoids at 50% probability. Hydrogen atoms are omitted for clarity.

Ru aqua/hydroxyl complexes. That is why the PCET reaction rate k_2 is not significantly affected.

The Ru–O_2N_2–N_2 analogues

Tetradentate O^N^N^O ligands, such as H_2bda (2,2′-bipyridine-6,6′-dicarboxylic acid) and H_2pda (1,10-phenanthroline-2,9-dicarboxylic acid), were designed for preparing mononuclear Ru WOCs on the inspiration of the H_2cppd ligand. Thanks to the strong stabilization ability of anionic ligands on high-valent metal complexes, we were able to isolate a seven-coordinate Ru^{IV} intermediate of a Ru–bda WOC.

The Ru–bda WOCs. Complex $[Ru(bda)(pic)_2]$ (**12**, Figure 10) was synthesized via a two-step, one-pot reaction

DOI: 10.1021/acs.accounts.5b00149
Acc. Chem. Res. 2015, 48, 2084–2096

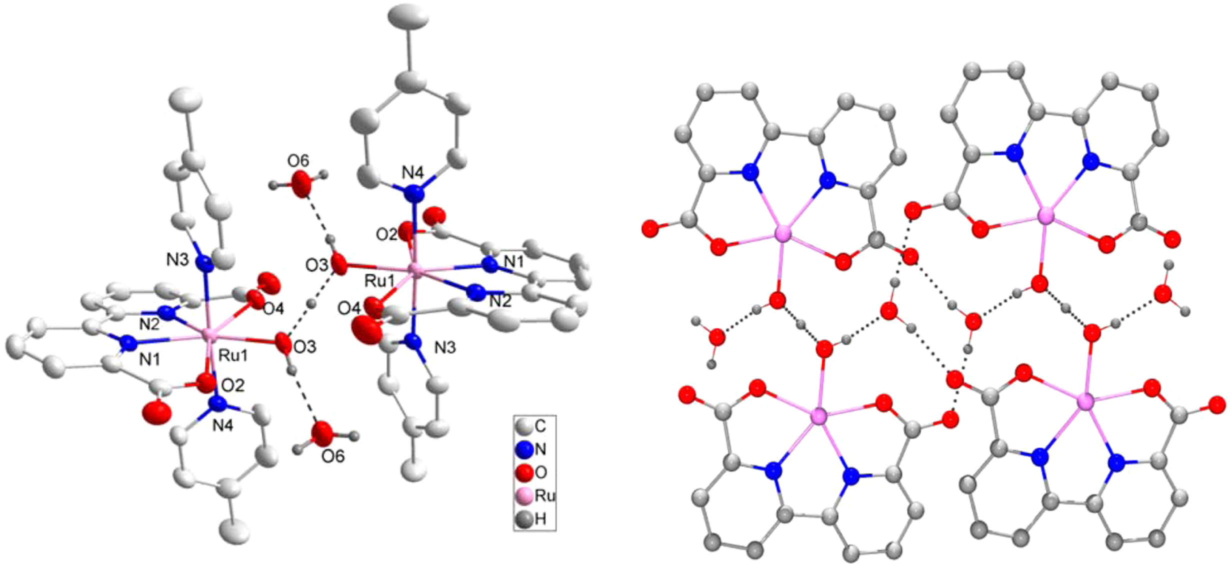

Figure 12. (left) The crystal structure of complex **12′** with thermal ellipsoids at 50% probability. Hydrogen atoms except the H−O type are omitted for clarity. (right) Illustration of the O−H···O hydrogen bonding network in the crystal structure (Pic ligands and hydrogen atoms except the H−O type are omitted for clarity).

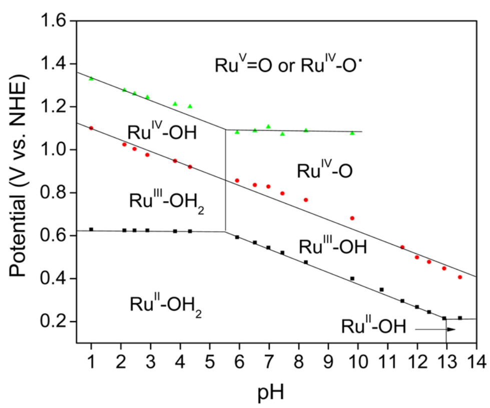

Figure 13. Pourbaix diagram of complex **12**.

in a moderate yield. The X-ray single crystal structure of **12** (Figure 11) revealed a wide cleft of O2−Ru1−O3 (122.99°), which is essential for accepting a water molecule to coordinate with the Ru center.[16]

Electrochemistry study on **12** suggested that the Ru^{IV} state is thermodynamically stable under pH 1.0 conditions, which allowed us to isolate the Ru^{IV} species as a seven-coordinate dimeric complex μ-(HOHOH)[Ru^{IV}(bda)(pic)$_2$]$_2$[PF_6]$_3$·(**12′**) (Figure 12, left) with two solvated water molecules.[16] Each Ru center is in seven coordination with a distorted pentagonal bipyramidal configuration. Each solvated water molecule hydrogen bonds with the $[HOHOH]^-$ bridge and two carboxylate O atoms (Figure 12, right), which stabilizes the binuclear complex in the solid state and meanwhile suggests a potential proton transfer path from the reaction center to the solvation shell via the basic site of carboxylate during water oxidation.

The Pourbaix diagram of **12** is depicted in Figure 13. Between pH 5.5 and pH 12.9, a $1e^-/1H^+$ proton-coupled electron transfer process was found for the $Ru^{III/II}$ couple. A $1e^-/1H^+$ PCET process was observed for the $Ru^{IV/III}$ process over the whole pH window (pH 1−13.5). Below pH 5.5, the oxidation of Ru^{IV}−OH to Ru^V═O is coupled with one proton transfer. On the basis of the Pourbaix diagram, a water molecule could coordinate to the Ru center of **12** in an aqueous solution, forming a $Ru^{II}-OH_2$ complex (most likely a six-coordinate species with a cleavage of other bonds). The subsequent proton/electron transfer events in the typical conditions of Ce^{IV}-driven water oxidation (pH < 2) was proposed as follows: $Ru^{II}-OH_2 \rightarrow Ru^{III}-OH_2 \rightarrow Ru^{IV}-OH \rightarrow Ru^{V}{=}O$. Cyclic voltammogram measurements indicate that Ru^V═O triggers water oxidation.

Mechanistic Studies on **12** at pH 1.0 and under Stoichiometric Ce^{IV} conditions (by using stopped-flow technique) illustrated a catalytic cycle as shown in Figure 14.[17] The $[Ru^{II}-OH_2]$ is first oxidized to $[Ru^{III}-OH_2]^+$, followed by two $1H^+/1e^-$ PCET oxidation steps affording $[Ru^V{=}O]^+$ via $[Ru^{IV}-OH]^+$. The Ru^V oxo is in resonance with the Ru^{IV} oxyl radical. Thereafter, two Ru^V oxo units couple to each other, generating the peroxo intermediate $[Ru^{IV}-OO-Ru^{IV}]^{2+}$. The last step is oxygen release and regeneration of the catalyst, which is the RDS. The energy barrier for the O−O formation is only 11.9 kcal/mol based on DFT calculations.[18]

In the presence of excess Ce^{IV}, water oxidation by **12** is zero order in Ce^{IV} and second order in catalyst, suggesting the dimerization (the O−O bond formation step) is the RDS.[17] The oxygen liberation step under excess Ce^{IV} conditions is boosted in comparison with that under stoichiometric Ce^{IV} conditions. Accordingly, a fast oxidation of the peroxo intermediate $[Ru^{IV}-OO-Ru^{IV}]^{2+}$ to a superoxo-species ($[Ru^{IV}-O\dot{-}O-Ru^{IV}]^{3+}$) was proposed (calculated E^{ox} = 1.03 V) (eq 2). The oxygen liberation from the $[Ru^{IV}-O\dot{-}O-Ru^{IV}]^{3+}$ superoxo intermediate (eq 3) should be faster than that from the $[Ru^{IV}-OO-Ru^{IV}]^{2+}$ peroxo intermediate. As a result, the rate limiting step switches to the radical coupling step, in agreement with the second order dependence.

$$[Ru^{IV}-OO-Ru^{IV}]^{2+} + Ce^{IV} \xrightarrow{\text{fast}} [Ru^{IV}-O\dot{-}O-Ru^{IV}]^{3+} + Ce^{III} \quad (2)$$

$$[Ru^{IV}-O\dot{-}O-Ru^{IV}]^{3+} \xrightarrow{\text{fast}} Ru^{III} + Ru^{IV} + O_2 \quad (3)$$

DOI: 10.1021/acs.accounts.5b00149
Acc. Chem. Res. 2015, 48, 2084−2096

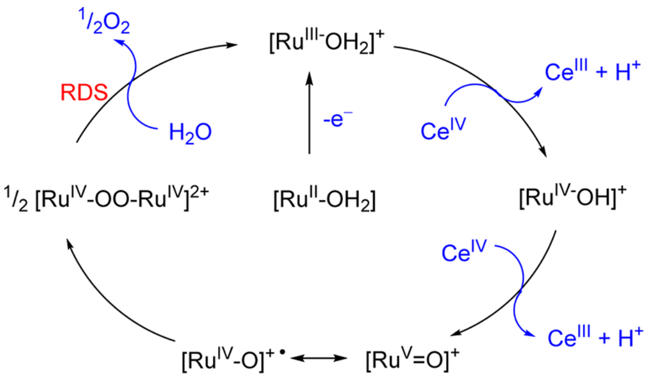

Figure 14. Proposed reaction mechanism for **12**-catalyzed water oxidation with stoichiometric oxidant.

Electronic and Hydrophobic Effects. A systematic installation of electron withdrawing and donating and hydrophobic and hydrophilic groups on the two axial pyridyl ligands was performed, and a series of mononuclear Ru complexes Ru(bda)L_2 (L = [$HNEt_3$][3-SO_3-pyridine], 4-(EtOOC)-pyridine, 4-bromopyridine, pyridine, 4-methoxypyridine, 4-(Me_2N)-pyridine and 4-[$Ph(CH_2)_3$]-pyridine) were prepared.[19] Electron withdrawing groups as well as hydrophobic groups displayed positive effects on the water oxidation reactivity. For instance, decent water oxidation activity was observed for the 4-(EtOOC)-pyridine coordinating Ru−bda catalyst (TON = 4800, $TOF_{initial}$ = 119 s^{-1}) and the 4-bromopyridine coordinating Ru−bda catalyst (TON = 4500, $TOF_{initial}$ = 115 s^{-1}).

The [Ru(bda)(isoq)$_2$] Complex. Since the RDS for **12** under catalytic conditions is the radical coupling step, enhancing the radical coupling step will increase its catalytic activity. A π-extended, hydrophobic isoquinoline (isoq) ligand was introduced to replace 4-picoline, yielding [Ru(bda)(isoq)$_2$] (**13a**; Figure 10).[17] There is a dramatic increase in TOF of **13a** (TOF = 303 ± 9.6 s^{-1} for **13a** versus 32 s^{-1} for **12**), which is attributed to noncovalent attractive interactions between isoquinolines, such as π−π stacking and hydrophobic effects, which lower the energy barrier of the coupling step. DFT calculations showed the important role of isoquinoline π−π stacking in stabilizing the transition state of the O−O bond formation step (Figure 15).[17]

Tuning the Longevity of Ru-bda WOCs. Axial ligand dissociation was identified as the major degradation pathway for the Ru-bda WOCs (Figure 16; axial ligand dissociation occurs more readily at the $Ru^V{=}O$ state). The dissociation energy was calculated on a series of ligands, including 4-picoline, pyrimidine, pyrazine, pyridazine, cinnoline, phthalazine, and 4,5-dimethoxypyridazine. A good correlation between the HOMO energy and the ligand dissociation energy was established.[20] As shown in Figure 17, Ru-bda WOCs with ligands at the upper-right corner should be more stable against ligand exchange than those with ligands at bottom-left corner.

Three complexes [Ru(bda)L_2] (L = pyrimidine (pmd), **14**; pyridazine (pdz), **15**; phthalazine (ptz), **16a**; Figure 10) were representatively prepared, and their longevities were compared with those of complexes **12** and **13a** (Table 2). In agreement with the prediction from Figure 17, the longevity of **15** and **16a** is notably better than that of complexes **12**, **13a**, and **14**. The TON of the most robust catalyst **16a** has reached over 55 000. For the future development of robust Ru-bda catalysts, one can just simply calculate the HOMO energy of a ligand to predict the longevity of the corresponding Ru-bda catalyst.

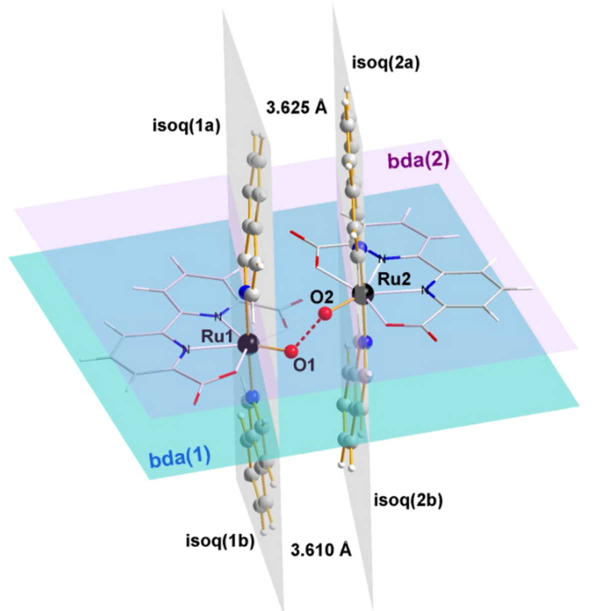

Figure 15. Calculated structure of the transition state of the radical O−O bonding, TS^{OO}(isoq) ([O1−O2] = 2.038 Å) of **13a**.

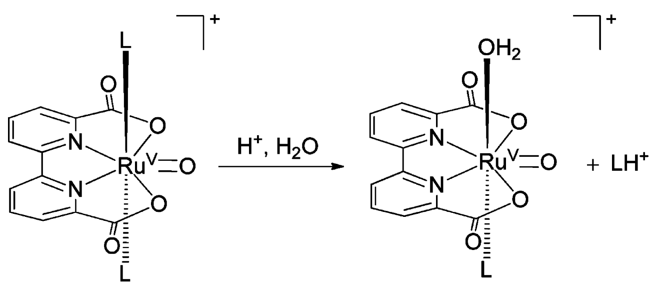

Figure 16. Illustration of the ligand exchange reaction studied in DFT calculations.

The Ru-bda WOCs with Halogen Substituted Axial Ligands. Both the electron withdrawing and the hydrophobic effects of axial ligands will enhance the activity of Ru-bda WOCs.[19] Thereby, we introduced halogen substitutes into the axial ligands of **13a** and **16a** and designed and prepared complexes **13b** and **16b** (Figure 10).[21] Notably, cosolvents, such as CH_3CN and CF_3CH_2OH, which were used to help dissolve catalysts in aqueous solutions, exhibited dramatic effect on the catalytic activity. The DFT calculation results disclosed that CH_3CN competes with H_2O in coordination with the Ru center and thus slows the catalytic rate of water oxidation, which however does not occur in the case of CF_3CH_2OH. When the less-coordinating cosolvent CF_3CH_2OH was used, complex **13b** showed a super high $\mathbf{TOF_{initial}}$ **> 1000 s^{-1}** and catalyst **16b** achieved an extraordinary high **TON > 100 000** under specific conditions. Both values are the highest recorded to date.

The [Ru(bda)(Imd)(dmso)] Analogues. Imidazole, which is present in the first coordination sphere of the Mn_4CaO_5 cluster,[3] is one of the important biological molecules. Several imidazole ligands were tested for building new Ru-bda catalysts, and C_s symmetric complexes [Ru^{II}(κ^3-bda)(dmso)L_2] (**17a−d**, L = imidazole-based ligand; in Figure 18) were obtained while 5-nitroimidazole led to [Ru^{II}(κ^4-bda)(5-nitroimidazole)$_2$] (**19a**).[22] For complexes **17a−d** in aqueous solutions, their equatorial imidazole ligands readily dissociate from their Ru

DOI: 10.1021/acs.accounts.5b00149
Acc. Chem. Res. 2015, 48, 2084−2096

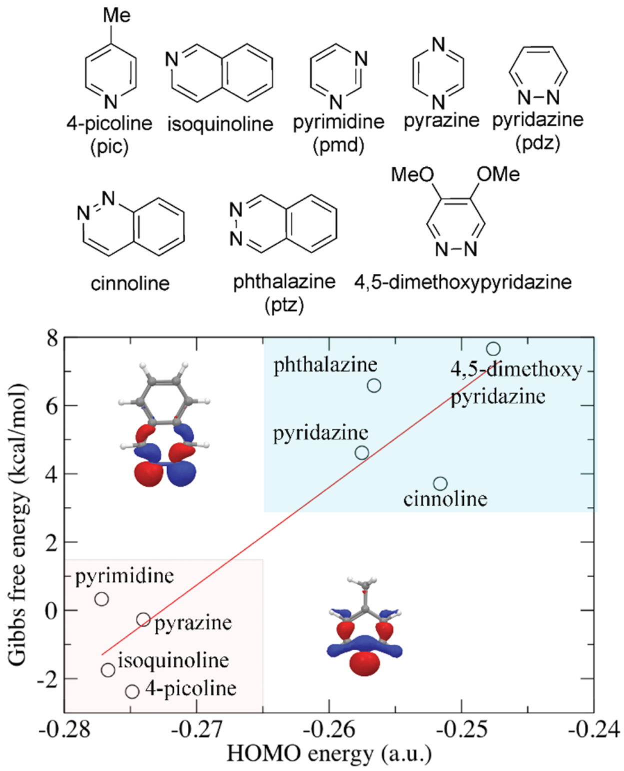

Figure 17. (top) Ligands screened in DFT calculations. The short names are given in the parentheses. (bottom) Gibbs free energy of reaction in pH 0.0 aqueous solution at 298 K as a function of HOMO energy of ligand in vacuum (in the insets are the HOMO orbital of 4-picoline and the HOMO − 1 orbital of phthalazine calculated with DFT).

Table 2. Longevity of Selected Ru−bda Catalysts under the Given Conditions and the Calculated Ligand Exchange Free Energy of Each Complex

complex	12	13a	14	15	16a
ΔG (kcal/mol)	−2.38	−1.75	0.33	4.61	6.59
longevity (h)[a]	0.29	0.064	0.332	1.07	1.37

[a]The longevity reported in this table is defined as the time when the oxygen production rate is 5% of the initial rate.

centers, yielding the corresponding Ru-bda catalysts [Ru^{II}(κ^4-bda)(dmso)L] (**18a−d**). This transformation was confirmed by crystallization of **17d**, which instead yielded **18d** as shown in Figure 19.

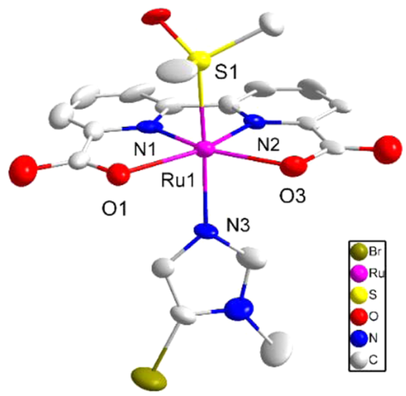

Figure 19. X-ray crystal structure of complex **18d** with thermal ellipsoids at 50% probability. Hydrogen atoms and solvated molecules are omitted for clarity.

The axially coordinated dmso ligand was found to greatly enhance the catalytic activity of the Ru-bda catalysts. For instance, complex **18d** gives a TOF of ∼170 s^{-1} while the analogous complex [Ru^{II}(κ^4-bda)(5-bromoimidazole)$_2$] (**19b**) lacking of the dmso ligand shows a TOF of ∼4 s^{-1} under the same conditions.

Similar to **12**, dmso-based catalysts also follow the binuclear reaction pathway by which two seven-coordinate Ru^V=O units couple to form the O−O bond. DFT calculations on the O−O bond formation were performed for both complexes **18d** and **19b**. The calculated potential energy profile of the O−O bond formation followed by the O_2-liberation shows that the axial ligand combination dmso/imidazole (**18d**) allows for unhindered coupling between terminal oxygen atoms of two Ru^V=O species, well accounting for the high O_2-evolution efficiency of **18d** compared with **19b**. The steric effect on catalytic enhancement is supposed to be more effective than the electronic effect.

Dinuclear Ru−bda WOCs. The intrinsic bimolecular coupling of Ru^V=O in the O−O bond formation step for Ru−bda catalysts limits their practical application on the electrode surface of a water-splitting device. A method to overcome this obstacle is forcing the intermolecular reaction to facile intramolecular reaction by covalently linking two or more catalytic units. As a proof of concept, three dinuclear ruthenium

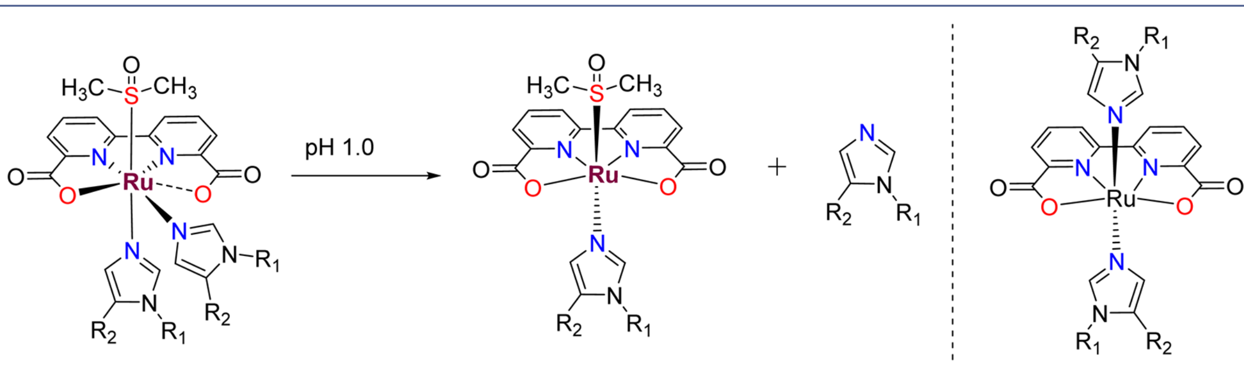

17a R_1, R_2=H
17b R_1=CH_3, R_2=H
17c R_1=H, R_2=CH_3
17d R_1=CH_3, R_2=Br

18a R_1, R_2=H
18b R_1=CH_3, R_2=H
18c R_1=H, R_2=CH_3
18d R_1=CH_3, R_2=Br

19a R_1=H, R_2=NO_2
19b R_1=CH_3, R_2=Br

Figure 18. Structures of complexes **17a−d**, **18a−d**, and **19a,b**, as well as the schematic formation of **18a−d** from **17a−d** at pH 1.0.

DOI: 10.1021/acs.accounts.5b00149
Acc. Chem. Res. 2015, 48, 2084−2096

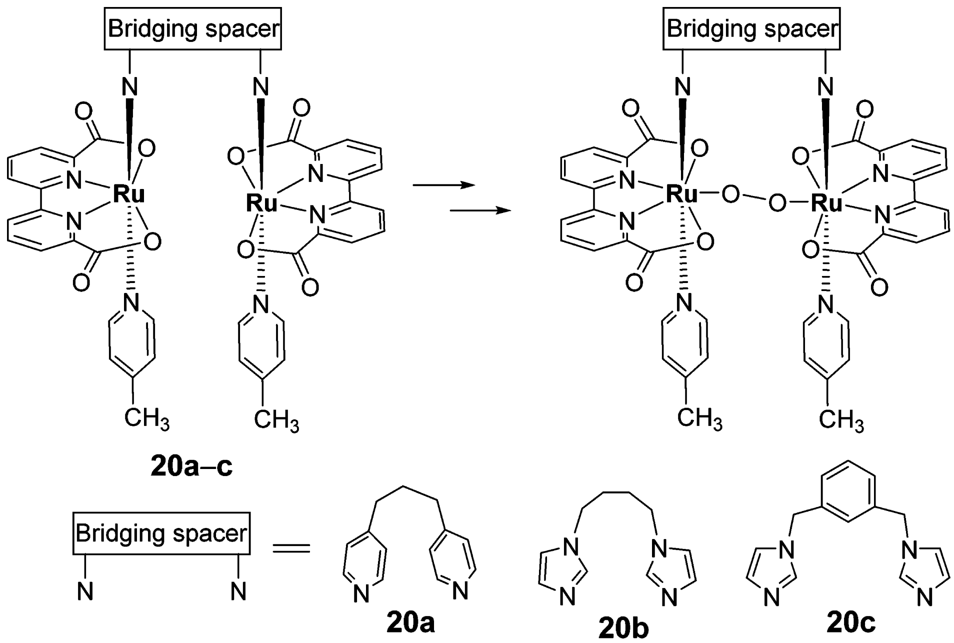

Figure 20. Structures of ruthenium dimer catalysts **20a–c**, as well as the proposed intramolecular O–O coupling.

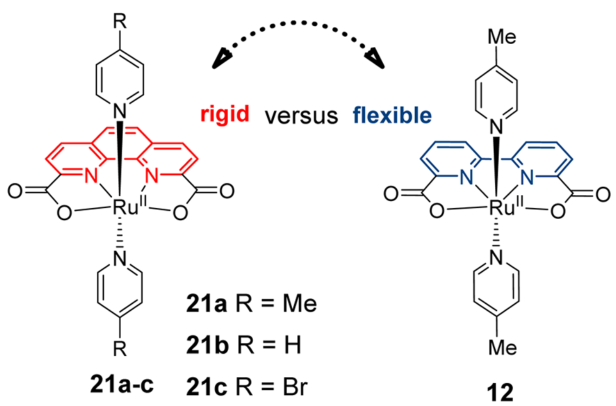

Figure 21. Molecular structures of **21a–c** versus **12**.

complexes, **20a–c** (Figure 20), with proper bridging spacers were prepared.[23] The use of soft spacer was thought to give rise to a flexible molecular cleft that can accommodate dynamically changed distances between ruthenium centers over the entire catalytic cycle.

The variation of either axial ligand or spacer had insignificant effect on the catalytic activity of Ce^{IV}-driven water oxidation. Complex **20c** bearing imidazole ligands and a $-CH_2-Ph-CH_2-$ spacer exhibited the best performance toward water oxidation. Seven-fold increase in oxygen evolution relative to the monomeric **12** was evidenced. Under a low concentration of **20c**, over 42000 turnovers were achieved in 1 h with a remarkable $TOF_{initial}$ of 40 s^{-1}. Meanwhile, the oxygen evolution rate shows first-order kinetics in catalyst, indicative of a single molecular reaction that involves an intramolecular O–O bond coupling pathway (Figure 20).

The Ru–pda WOCs. The bipyridyl backbone of the seven-coordinate Ru–bda intermediate is bent toward the Ru atom and twisted out of plane. Such ligand reorganization is to adapt the pentagonal bipyramidal configuration. The Ru–pda catalysts $[Ru(pda)L_2]$ (**21a–c**; Figure 21) with a rigid phenanthroline backbone motif were then designed to reveal the reorganization effect on water oxidation.[24]

Similar to the Ru–bda WOCs, a seven-coordinate Ru^{IV}–OH species $[Ru^{IV}(pda)(pic)_2(OH)]^+$ was also observed by mass spectrometry. Complexes **21a–c** are capable of catalyzing Ce^{IV}-driven water oxidation with fewer turnovers and lower turnover frequency than the Ru–bda one: 336 (0.092 s^{-1}) for **21a**, 310 (0.102 s^{-1}) for **21b**, and 190 (0.040 s^{-1}) for **21c**. Electron donating groups increase the catalytic activity of the Ru–pda complex. Interestingly, the oxygen evolution rate is first order in catalysts **21a–c** in comparison with a second order kinetics of **12**, implying a mononuclear catalytic pathway and an O–O bond formation pathway via water nucleophilic attack on a metal–oxo complex. The electrochemistry study showed that Ru^V=O triggers the O–O bond formation, and DFT calculations revealed that the energy barrier of the water nucleophilic attack path (13.3 kcal/mol) is lower than the Ru^V=O coupling path (16.4 kcal/mol) by 3.1 kcal/mol. A shift of the Ru^{III} atom toward one side of the pda^{2-} cavity occurs in the transition state of the WNA path of $[O{=}Ru^V(pda)(py)_2]^+$ (py = pyridine; the axial 4-picoline ligands were replaced by the pyridine ligands in the DFT calculations), resulting in the cleavage of one $Ru-O_{carboxylate}$ bond, because the pda^{2-} ligand is big and rigid and cannot accommodate the Ru^{III} well.

BRIEF ACCOUNTS OF VISIBLE-LIGHT-DRIVEN WATER OXIDATION SYSTEMS AND FUNCTIONAL DEVICES

Studying Ce^{IV}-driven water oxidation is one efficient means to evaluate the catalyst activity. Good catalysts could be then selected for further applications, such as constructing light-driven water oxidation systems and functional water splitting devices.

Homogeneous Visible Light-Driven Water Oxidation

The negatively charged ligands have drastically improved the catalytic efficiency and lowered the oxidation potentials of Ru-based WOCs. Especially, the catalytic onset potential of our Ru-based WOCs was considerably decreased, which allowed us to incorporate many photosensitizers to drive water oxidation by using visible light.[25−27] Figure 22 representatively presents a

DOI: 10.1021/acs.accounts.5b00149
Acc. Chem. Res. 2015, 48, 2084−2096

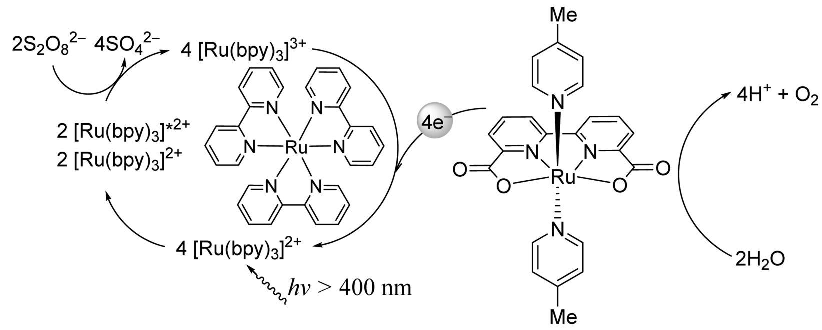

Figure 22. Working principle of visible light-driven water oxidation representatively using **12**.

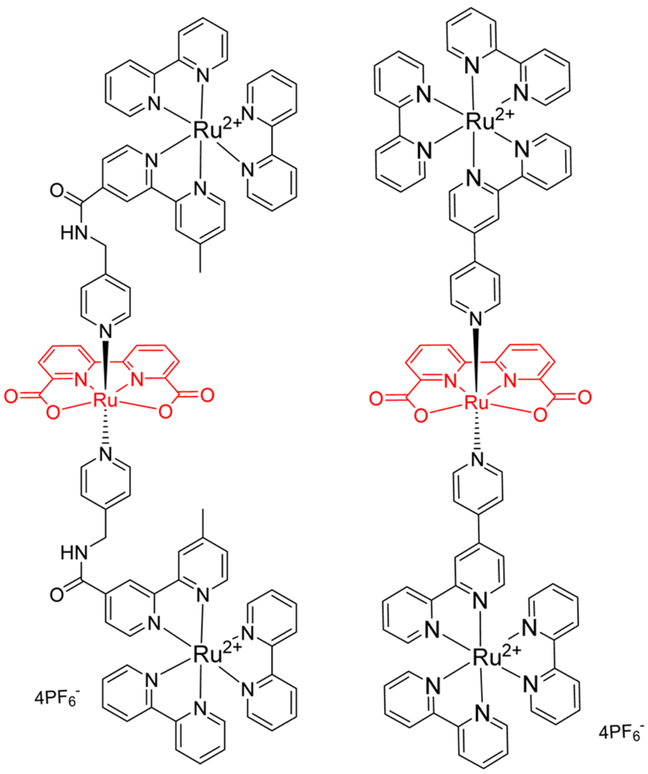

Figure 23. Molecular structures of two photosensitizer−catalyst assemblies.

typical visible light-driven water oxidation system consisting of three components: a WOC, a photosensitizer and a sacrificial electron acceptor.[28] Besides, supramolecular assemblies where photosensitizer is linked covalently with a catalyst were also demonstrated to be capable of catalyzing water oxidation under visible light irradiation (Figure 23).[29,30]

Water Oxidation Devices

For practical applications, catalysts have to be fabricated on the electrode surface and split water using either electric or solar power.

Water Oxidation Anode. Our Ru catalysts have been assembled on different electrodes via several methods, such as the direct C−C bond linkage,[31] $\pi-\pi$ stacking between multiwall carbon nanotubes and pyrene units of catalyst, and the hydrophobic force between carbon nanotubes and long alkyl chains of catalyst (Figure 24).[32,33]

Photoanode for Water Oxidation. The Ru^{III} species of **12**, namely $[\mathbf{12}]^+$, is integrated by Nafion (due to electrostatic interaction between anionic sulfonate of Nafion and cationic $[\mathbf{12}]^+$) with dye-sensitized TiO_2 film, and the resulting photoanode is active for water splitting.[34] More durable devices were obtained by introducing proper anchoring groups, such as phosphonic acid, silane, and dipicolinic acid groups, to WOCs, which can be tethered on the semiconductor materials (Figure 25), resulting in photoresponsive anodes for water oxidation.[35−37]

■ CONCLUSION AND PERSPECTIVE

Negatively charged ligands have been successfully introduced to prepare efficient Ru WOCs and a few of those Ru WOCs with low overpotential have been employed for light driven water splitting systems, as well as the fabrication of water oxidation anodes. The negatively charged ligands stabilize high valent

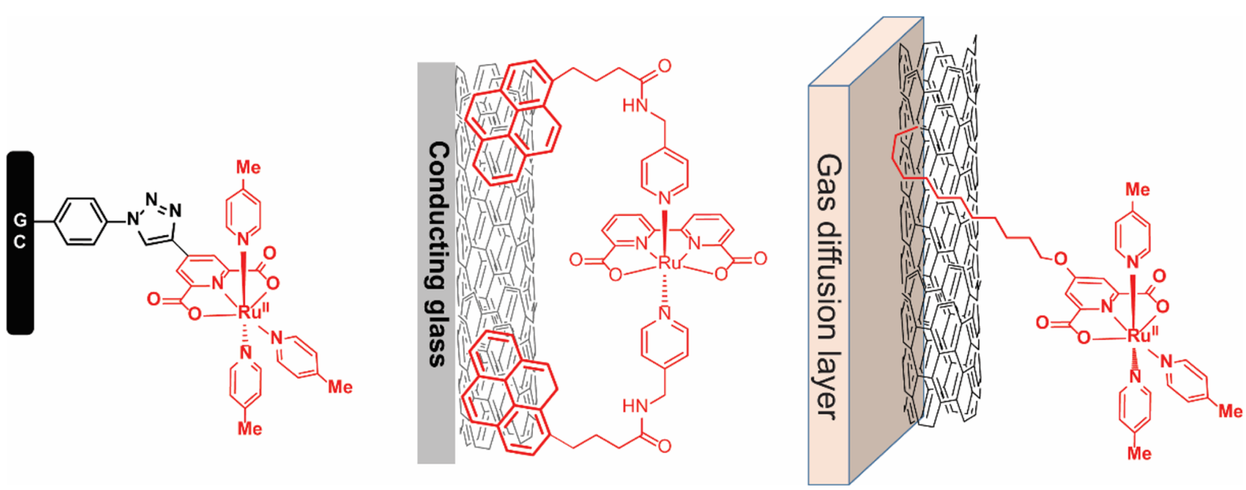

Figure 24. Representative illustration of three electrodes functionalized with Ru WOCs.

DOI: 10.1021/acs.accounts.5b00149
Acc. Chem. Res. 2015, 48, 2084−2096

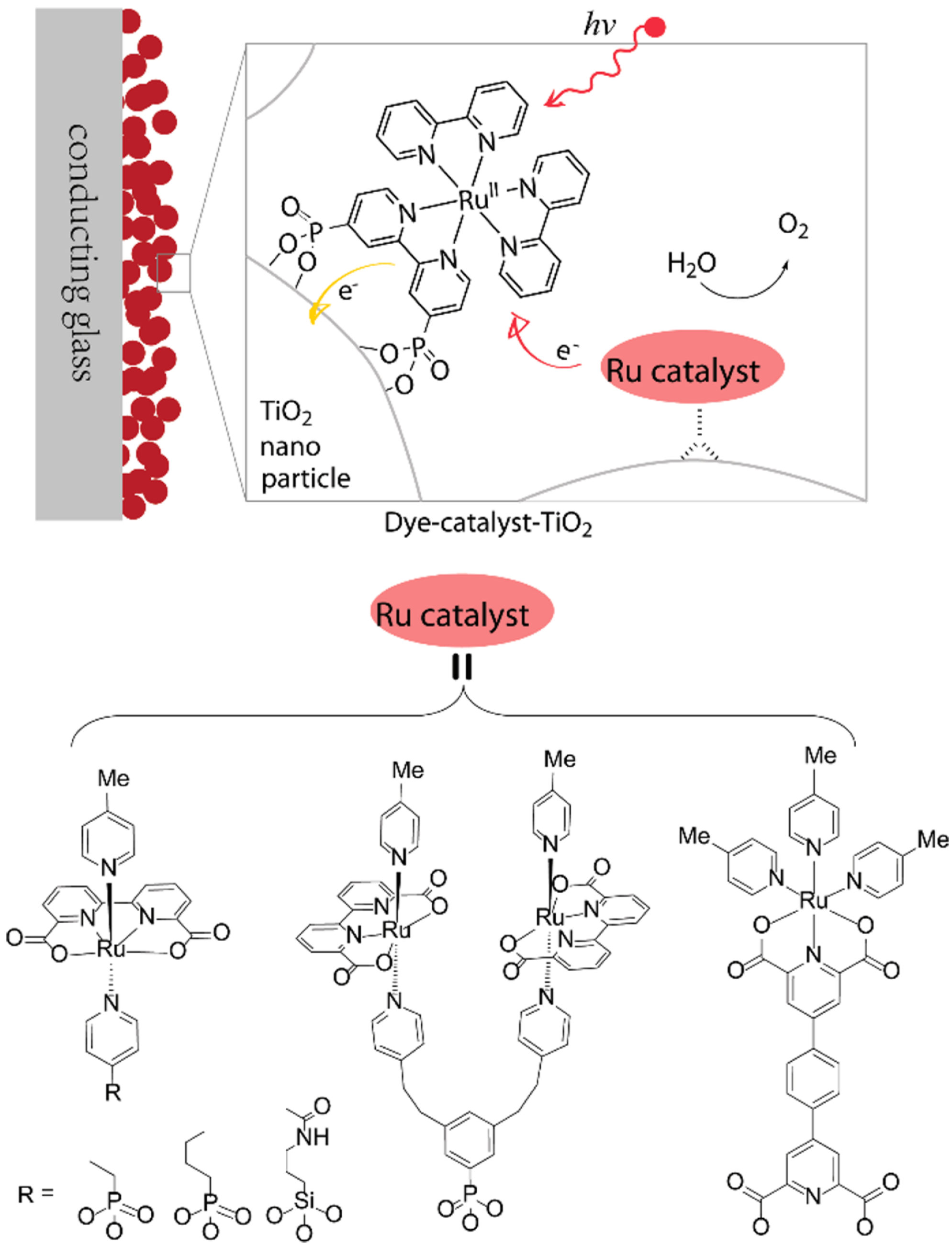

Figure 25. Representative illustration of photoanodes for light driven water splitting.

metal complexes, which significantly reduces the oxidation potentials of Ru complexes as well as the overpotential toward water oxidation. Meanwhile, the negatively charged, strong electron donating ligands facilitate the ligand exchange process of the metal complexes, which may also facilitate oxygen release from the metal center. The water oxidation mechanisms by those Ru catalysts are different when different auxiliary ligands are involved. Particularly, the Ru−bda WOCs catalyze the O−O bond formation via the radical coupling mechanism, while many other WOCs catalyze the O−O bond formation through the water nucleophilic attack pathway. Apparently, the Ru−bda catalysts are much faster than those catalysts using the water nucleophilic attack mechanism. Understanding the factors that control the radical coupling path is required to design new catalysts that effectively catalyze water oxidation via the radical coupling mechanism. A coin has two sides, and the same is true for the negatively charged, strongly electron donating ligands. The negatively charged ligands can lower the oxidation potentials dramatically for the electron-transfer process while the effect becomes complicated to predict when a proton-coupled electron transfer process is involved. This is because strong electron donating ligands increase the pK_a of the metal−OH_2/metal−OH, making the proton dissociation comparably difficult to occur. Nowadays, DFT calculations are playing vital roles in understanding reaction mechanisms and designing new generation catalysts. With the aid of theoretical calculations, we have demonstrated the DFT-directed development of robust Ru−bda WOCs. Our concept on catalyst design might be applicable to the biomimetic catalysts based on earth-abundant metals.

For future large scale applications, the lifetime of current WOCs has to be further improved to increase their durability.

DOI: 10.1021/acs.accounts.5b00149
Acc. Chem. Res. 2015, 48, 2084−2096

Many strategies could be used to achieve more durable catalysts: (1) introduce all-inorganic template ligands to avoid the involvement of organic ligands, (2) immobilize catalysts on different electrode materials and insulate catalyst molecules from each other to decrease the intermolecular oxidative decomposition, and (3) increase the turnover frequency of the catalyst to minimize the oxidative decomposition side reactions. The stability issue is one of the most challenging tasks that chemists are facing now, and more attention should be paid to solve the stability issue.

■ AUTHOR INFORMATION

Corresponding Author

*E-mail: lichengs@kth.se.

Notes

The authors declare no competing financial interest.

Biographies

Lele Duan is a researcher at KTH Royal Institute of Technology. After receiving his Ph.D. degree under the supervision of Professor Licheng Sun at KTH in 2011, he started his postdoctoral career in the same group and later in 2013 joined in the Etsuko Fujita group at Brookhaven National Laboratory. His current research focuses on the development of artificial photosynthetic systems for fuel production.

Lei Wang is a graduate student under the supervision of Professor Licheng Sun in Department of Chemistry at KTH. His research focuses on the development of molecular WOCs and water splitting devices.

Fusheng Li joined the group of Professor Licheng Sun at KTH as a Ph.D. student in September 2011. He focuses on the design of molecular devices for both electrodriven and light-driven water splitting.

Fei Li is an associate professor at Dalian University of Technology (DUT), China. His research interests include photocatalytic and electrocatalytic water splitting with molecular catalysts.

Licheng Sun is a full Professor at KTH Royal Institute of Technology and a distinguished professor at DUT. His research interests cover solar cells and solar fuels, in particular, artificial photosynthesis, bioinspired water oxidation using molecular catalysts, and hydrogen generation using FeFe-hydrogenase model complexes. In addition, he is also interested in the development of photoelectrochemical cells based on molecular catalysts and nanostructured semiconductors.

■ ACKNOWLEDGMENTS

We are most grateful to present and past Sun group members, especially Dr. Yunhua Xu, for their great contributions to this Account. Finance is supported by the Swedish Research Council, the Swedish Energy Agency, the Knut & Alice Wallenberg Foundation, the National Natural Science Foundation of China (Grants 21120102036 and 91233201), the National Basic Research Program of China (973 program, 2014CB239402), and the China Scholarship Council.

■ REFERENCES

(1) Askerka, M.; Wang, J.; Brudvig, G. W.; Batista, V. S. Structural Changes in the Oxygen-Evolving Complex of Photosystem II Induced by the S1 to S2 Transition: A Combined XRD and QM/MM Study. *Biochemistry* **2014**, *53*, 6860−6862.

(2) Dismukes, G. C.; Brimblecombe, R.; Felton, G. A. N.; Pryadun, R. S.; Sheats, J. E.; Spiccia, L.; Swiegers, G. F. Development of Bioinspired Mn_4O_4−Cubane Water Oxidation Catalysts: Lessons from Photosynthesis. *Acc. Chem. Res.* **2009**, *42*, 1935−1943.

(3) Umena, Y.; Kawakami, K.; Shen, J.-R.; Kamiya, N. Crystal Structure of Oxygen-Evolving Photosystem II at A Resolution of 1.9 Å. *Nature* **2011**, *473*, 55−60.

(4) Wada, T.; Tsuge, K.; Tanaka, K. Electrochemical Oxidation of Water to Dioxygen Catalyzed by the Oxidized Form of the Bis(ruthenium−hydroxo) Complex in H_2O. *Angew. Chem., Int. Ed.* **2000**, *39*, 1479−1482.

(5) Zong, R.; Thummel, R. P. A New Family of Ru Complexes for Water Oxidation. *J. Am. Chem. Soc.* **2005**, *127*, 12802−12803.

(6) Gilbert, J. A.; Eggleston, D. S.; Murphy, W. R.; Geselowitz, D. A.; Gersten, S. W.; Hodgson, D. J.; Meyer, T. J. Structure and Redox Properties of the Water-Oxidation Catalyst $[(bpy)_2(OH_2)RuORu(OH_2)(bpy)_2]^{4+}$. *J. Am. Chem. Soc.* **1985**, *107*, 3855−3864.

(7) Xu, Y.; Duan, L.; kermark, T.; Tong, L.; Lee, B.-L.; Zhang, R.; kermark, B.; Sun, L. Synthesis and Catalytic Water Oxidation Activities of Ruthenium Complexes Containing Neutral Ligands. *Chem.—Eur. J.* **2011**, *17*, 9520−9528.

(8) Sun, L.; Hammarström, L.; Åkermark, B.; Styring, S. Towards Artificial Photosynthesis: Ruthenium−Manganese Chemistry for Energy Production. *Chem. Soc. Rev.* **2001**, *30*, 36−49.

(9) Huang, P.; Magnuson, A.; Lomoth, R.; Abrahamsson, M.; Tamm, M.; Sun, L.; van Rotterdam, B.; Park, J.; Hammarström, L.; Åkermark, B.; Styring, S. Photo-Induced Oxidation of A Dinuclear $Mn_2^{II,II}$ Complex to the $Mn_2^{III,IV}$ State by Inter- and Intramolecular Electron Transfer To Ru^{III}tris-Bipyridine. *J. Inorg. Biochem.* **2002**, *91*, 159−172.

(10) Xu, Y.; Aakermark, T.; Gyollai, V.; Zou, D.; Eriksson, L.; Duan, L.; Zhang, R.; Aakermark, B.; Sun, L. A New Dinuclear Ruthenium Complex as an Efficient Water Oxidation Catalyst. *Inorg. Chem.* **2009**, *48*, 2717−2719.

(11) Xu, Y.; Fischer, A.; Duan, L.; Tong, L.; Gabrielsson, E.; Åkermark, B.; Sun, L. Chemical and Light-Driven Oxidation of Water Catalyzed by an Efficient Dinuclear Ruthenium Complex. *Angew. Chem., Int. Ed.* **2010**, *49*, 8934−8937.

(12) Duan, L.; Xu, Y.; Gorlov, M.; Tong, L.; Andersson, S.; Sun, L. Chemical and Photochemical Water Oxidation Catalyzed by Mononuclear Ruthenium Complexes with a Negatively Charged Tridentate Ligand. *Chem.—Eur. J.* **2010**, *16*, 4659−4668.

(13) An, J.; Duan, L.; Sun, L. Ru Complexes Containing Pyridine Dicarboxylate Ligands: Electronic Effects on Their Catalytic Activity toward Water Oxidation. *Faraday Discuss.* **2012**, *155*, 267−275.

(14) Tong, L.; Wang, Y.; Duan, L.; Xu, Y.; Cheng, X.; Fischer, A.; Ahlquist, M. S. G.; Sun, L. Water Oxidation Catalysis: Influence of Anionic Ligands upon the Redox Properties and Catalytic Performance of Mononuclear Ruthenium Complexes. *Inorg. Chem.* **2012**, *51*, 3388−3398.

(15) Tong, L.; Inge, A. K.; Duan, L.; Wang, L.; Zou, X.; Sun, L. Catalytic Water Oxidation by Mononuclear Ru Complexes with an Anionic Ancillary Ligand. *Inorg. Chem.* **2013**, *52*, 2505−2518.

(16) Duan, L.; Fischer, A.; Xu, Y.; Sun, L. Isolated Seven-Coordinate Ru(IV) Dimer Complex with $[HOHOH]^-$ Bridging Ligand as an Intermediate for Catalytic Water Oxidation. *J. Am. Chem. Soc.* **2009**, *131*, 10397−10399.

(17) Duan, L.; Bozoglian, F.; Mandal, S.; Stewart, B.; Privalov, T.; Llobet, A.; Sun, L. A Molecular Ruthenium Catalyst with Water-Oxidation Activity Comparable to that of Photosystem II. *Nat. Chem.* **2012**, *4*, 418−423.

(18) Nyhlén, J.; Duan, L.; Åkermark, B.; Sun, L.; Privalov, T. Evolution of O_2 in a Seven-Coordinate Ru^{IV} Dimer Complex with a $[HOHOH]^{-1}$ Bridge: A Computational Study. *Angew. Chem., Int. Ed.* **2010**, *49*, 1773−1777.

(19) Duan, L.; Wang, L.; Inge, A. K.; Fischer, A.; Zou, X.; Sun, L. Insights into Ru-Based Molecular Water Oxidation Catalysts: Electronic and Noncovalent-Interaction Effects on Their Catalytic Activities. *Inorg. Chem.* **2013**, *52*, 7844−7852.

(20) Duan, L.; Araujo, C. M.; Ahlquist, M. S. G.; Sun, L. Highly Efficient and Robust Molecular Ruthenium Catalysts for Water Oxidation. *Proc. Natl. Acad. Sci. U. S. A.* **2012**, *109*, 15584−15588.

DOI: 10.1021/acs.accounts.5b00149
Acc. Chem. Res. 2015, 48, 2084−2096

(21) Wang, L.; Duan, L.; Wang, Y.; Ahlquist, M. S. G.; Sun, L. Highly Efficient and Robust Molecular Water Oxidation Catalysts Based on Ruthenium Complexes. *Chem. Commun.* **2014**, *50*, 12947−12950.

(22) Wang, L.; Duan, L.; Stewart, B.; Pu, M.; Liu, J.; Privalov, T.; Sun, L. Toward Controlling Water Oxidation Catalysis: Tunable Activity of Ruthenium Complexes with Axial Imidazole/DMSO Ligands. *J. Am. Chem. Soc.* **2012**, *134*, 18868−18880.

(23) Jiang, Y.; Li, F.; Zhang, B.; Li, X.; Wang, X.; Huang, F.; Sun, L. Promoting the Activity of Catalysts for the Oxidation of Water with Bridged Dinuclear Ruthenium Complexes. *Angew. Chem., Int. Ed.* **2013**, *52*, 3398−3401.

(24) Tong, L.; Duan, L.; Xu, Y.; Privalov, T.; Sun, L. Structural Modifications of Mononuclear Ruthenium Complexes: A Combined Experimental and Theoretical Study on the Kinetics of Ruthenium-Catalyzed Water Oxidation. *Angew. Chem., Int. Ed.* **2011**, *50*, 445−449.

(25) Duan, L.; Tong, L.; Xu, Y.; Sun, L. Visible Light-Driven Water Oxidation-From Molecular Catalysts to Photoelectrochemical Cells. *Energy Environ. Sci.* **2011**, *4*, 3296−3313.

(26) Xu, Y.; Duan, L.; Tong, L.; Aakermark, B.; Sun, L. Visible Light-Driven Water Oxidation Catalyzed by A Highly Efficient Dinuclear Ruthenium Complex. *Chem. Commun.* **2010**, *46*, 6506−6508.

(27) Wang, L.; Duan, L.; Tong, L.; Sun, L. Visible Light-Driven Water Oxidation Catalyzed by Mononuclear Ruthenium Complexes. *J. Catal.* **2013**, *306*, 129−132.

(28) Duan, L.; Xu, Y.; Zhang, P.; Wang, M.; Sun, L. Visible Light-Driven Water Oxidation by a Molecular Ruthenium Catalyst in Homogeneous System. *Inorg. Chem.* **2010**, *49*, 209−215.

(29) Wang, L.; Mirmohades, M.; Brown, A.; Duan, L.; Li, F.; Daniel, Q.; Lomoth, R.; Sun, L.; Hammarström, L. Sensitizer-Catalyst Assemblies for Water Oxidation. *Inorg. Chem.* **2015**, *54*, 2742−2751.

(30) Li, F.; Jiang, Y.; Zhang, B.; Huang, F.; Gao, Y.; Sun, L. Towards a Solar Fuel Device: Light-Driven Water Oxidation Catalyzed by a Supramolecular Assembly. *Angew. Chem., Int. Ed.* **2012**, *51*, 2417−2420.

(31) Tong, L.; Goethelid, M.; Sun, L. Oxygen Evolution at Functionalized Carbon Surfaces: A Strategy for Immobilization of Molecular Water Oxidation Catalysts. *Chem. Commun.* **2012**, *48*, 10025−10027.

(32) Li, F.; Zhang, B.; Li, X.; Jiang, Y.; Chen, L.; Li, Y.; Sun, L. Highly Efficient Oxidation of Water by a Molecular Catalyst Immobilized on Carbon Nanotubes. *Angew. Chem., Int. Ed.* **2011**, *50*, 12276−12279.

(33) Li, F.; Li, L.; Tong, L.; Daniel, Q.; Gothelid, M.; Sun, L. Immobilization of A Molecular Catalyst on Carbon Nanotubes for Highly Efficient Electro-Catalytic Water Oxidation. *Chem. Commun.* **2014**, *50*, 13948−13951.

(34) Li, L.; Duan, L.; Xu, Y.; Gorlov, M.; Hagfeldt, A.; Sun, L. A Photoelectrochemical Device for Visible Light Driven Water Splitting by A Molecular Ruthenium Catalyst Assembled on Dye-Sensitized Nanostructured TiO_2. *Chem. Commun.* **2010**, *46*, 7307−7309.

(35) Gao, Y.; Ding, X.; Liu, J.; Wang, L.; Lu, Z.; Li, L.; Sun, L. Visible Light Driven Water Splitting in a Molecular Device with Unprecedentedly High Photocurrent Density. *J. Am. Chem. Soc.* **2013**, *135*, 4219−4222.

(36) Fan, K.; Li, F.; Wang, L.; Daniel, Q.; Gabrielsson, E.; Sun, L. Pt-Free Tandem Molecular Photoelectrochemical Cells for Water Splitting Driven by Visible Light. *Phys. Chem. Chem. Phys.* **2014**, *16*, 25234−25240.

(37) Zhang, L.; Gao, Y.; Ding, X.; Yu, Z.; Sun, L. High-Performance Photoelectrochemical Cells Based on a Binuclear Ruthenium Catalyst for Visible-Light-Driven Water Oxidation. *ChemSusChem* **2014**, *7*, 2801−2804.

DOI: 10.1021/acs.accounts.5b00149
Acc. Chem. Res. 2015, 48, 2084−2096